

Early Dynamics of Deep Blue XBT Probes

FRANCIS BRINGAS AND GUSTAVO GONI

National Oceanic and Atmospheric Administration/Atlantic Oceanographic and Meteorological Laboratory, Miami, Florida

(Manuscript received 12 March 2015, in final form 23 September 2015)

ABSTRACT

Expendable bathythermographs (XBTs) are probes widely used to monitor global ocean heat content, variability of ocean currents, and meridional heat transports. In the XBT temperature profile, the depth is estimated from the time of descent in the water using a fall-rate equation. There are two main errors in these profiles: temperature and depth errors. The reduction of error in the estimates of the depth allows a corresponding reduction in the errors in the computations in which XBTs are used. Two experiments were carried out to study the effect of the deployment height on the depth estimates of Deep Blue XBT probes. During these experiments, XBTs were deployed from different heights. The motion of the probes after entering the water was analyzed to determine the position and the velocity of the probes as a function of time, which was compared to that obtained using the Hanawa et al. fall-rate equation. Results showed a difference or offset between the experimentally observed depths and those derived from Hanawa et al. This offset was found to be linked to the deployment height. To eliminate the offset in the fall-rate equation for XBTs deployed from different heights, a methodology is proposed here based on the initial velocities of the probes in the water (or deployment height). Results indicate that the depth estimates in the profiles need to be corrected for an offset, which in addition to having a launch height dependence is time dependent during the first 1.5 s of descent of the probe in the water, and constant after that.

1. Introduction

Expendable bathythermographs (XBTs) are widely used to measure temperature profiles since their introduction several decades ago. Currently, approximately 20 000 XBTs are globally deployed along fixed transects every year from ships of opportunity and research vessels. Typically, the deployments are made from different heights up to approximately 25 m, at ship speeds between 0 and 25 kt (1 kt = 0.514 m s⁻¹). The temperature is determined with a thermistor whose signal is transmitted to the recorder on board the ship through a wire that spools out of the probe, constituting the main limitation to the maximum depth that can be reached. Since the probes do not have pressure sensors, the depth is determined by a semiempirical relation $z(t)$ of the form (Green 1984),

$$z(t) = at - bt^2, \quad (1)$$

known as the fall-rate equation (FRE), where the coefficients a and b are determined empirically for different types of XBT probes. These two coefficients are defined using a dynamical model describing the movement of the XBT in the water as the result of a force balance between the hydrodynamic drag, the decreasing buoyancy caused by the wire loss, and the increase of seawater viscosity with depth (Green 1984; Hallock and Teague 1992, hereafter HT92). The coefficient a represents the terminal velocity of the XBT in the seawater, while the coefficient b represents a deceleration introduced as a correction to the first term in (1) as a result of the loss of weight of the probe as the wire is spooled out. Since $b \ll a$, according to the FRE the XBTs fall at an almost constant velocity throughout their descent in the water. When the vertical axis is defined as positive downward, both coefficients are positive. The original values of coefficients a and b used for the Deep Blue type of XBTs were 6.472 m s⁻¹ and 0.002 16 m s⁻², respectively (NOAA 2014, code 51).

There are several sources of error that may affect the accuracy in temperature and depth of the XBT profile

Corresponding author address: Francis Bringas, National Oceanic and Atmospheric Administration/Atlantic Oceanographic and Meteorological Laboratory, 4301 Rickenbacker Causeway, Miami, FL 33149.
E-mail: francis.bringas@noaa.gov

(Cowley et al. 2013). The work presented here focuses on depth offsets using the XBT FRE estimates. The XBT fall rate, determined by (1), has been the subject of numerous studies since the 1980s, which included reports on systematic errors in the depth estimates (Seaver and Kuleshov 1982; Roemmich and Cornuelle 1987). The impact that these depth errors may have in climate research was later recognized from a comprehensive analysis carried out using CTD and XBT data in several regions (Hanawa et al. 1995, hereafter H95), where new coefficients a and b were estimated as

$$a = 6.691 \text{ m s}^{-1}; \quad b = 0.00225 \text{ m s}^{-2}. \quad (2)$$

New advances in the research of XBT FRE biases indicated that these biases are time dependent (Gouretski and Koltermann 2007). This inspired a large number of studies to determine the cause of these biases, to assess their values, and to propose correction schemes for XBT data. These corrections have been obtained using a suite of different methods, including XBT–CTD comparisons (Seaver and Kuleshov 1982; Heinmiller et al. 1983; Hanawa and Yoritaka 1987; Singer 1990; HT92; Thadathil et al. 2002; Reseghetti et al. 2007; Wijffels et al. 2008; Ishii and Kimoto 2009; Levitus et al. 2009; Gouretski and Reseghetti 2010; DiNezio and Goni 2011; Kizu et al. 2011; Hamon et al. 2012; Cowley et al. 2013; Cheng et al. 2015) and XBT and altimetry, (DiNezio and Goni 2010) among others. In particular, some of these studies generally reported the presence of depth offsets without a clear indication of the physical mechanisms that caused these offsets. For example, using a statistical analysis of a large number of side-by-side XBT–CTD pairs, Cowley et al. (2013) found that in their linear model for depth bias, the offset term appears to compensate for an acceleration over the upper 100 m. Reseghetti et al. (2007) also analyzed collocated XBT–CTD pairs, with XBTs deployed from different initial heights. While the possible effect of the deployment height and the verticality of the probe while entering the water were discussed in their work as possible factors to cause a depth offset in the XBT profile, their results provided uncertain indications of the influence of the deployment height on the motion of the probes during the first few meters in the water. Other factors, such as the response time of the acquisition system, were found to have a greater impact on the XBT profiles in the near-surface layer. DiNezio and Goni (2010) estimated systematic biases between XBT and Argo observations using satellite altimetry. In this case depth offsets in the upper meters were found to be different among ocean basins, which made the authors unable to identify systematic errors in the FRE resulting from transients in the initial descent of the probes. Although many

efforts and methodologies address XBT biases originated by the fall-rate coefficient discrepancies, few experiments (e.g., HT92; Xiao et al. 2006) and numerical simulations (e.g., Abraham et al. 2012a; Abraham et al. 2012b; Xiao and Zhang 2012) have been conducted to assess the dynamic characteristics of the XBT during the first few meters of movement in the water. During this short distance after the XBT hits the water, the probe may not yet be moving at its terminal velocity, as prescribed by the most commonly used FREs. Thus, it could be expected that the first few meters of movement may significantly contribute to a potential depth offset in the temperature profile as estimated by most FREs.

Because of the extensive use of XBTs in ocean current monitoring (e.g., Carton and Katz 1990; Goni et al. 1996; Gilson et al. 1998; Arnault et al. 1999, 2011; Phillips and Rintoul 2002; Rintoul et al. 2002; Ridgway et al. 2008; Gourcuff et al. 2011; Goes et al. 2013; Domingues et al. 2014; Dong et al. 2009, 2014; Goes et al. 2015), and to determine the ocean thermal structure and heat transport (Smith et al. 1999; Roemmich et al. 2001; Baringer and Garzoli 2007; Abraham et al. 2013; Dong et al. 2009), as well as their remarkable contribution to the knowledge we have about the ocean today, it is critical to properly assess the fall-rate equation coefficients to improve historical XBT datasets and to establish standards for current and future observations.

This work reports two experiments carried out with the goal to study the main characteristics of the Sippican Deep Blue XBT rate of descent during the first 11 m after entering the water. The objectives of these experiments were 1) to determine the time it takes for the XBTs, which are entering the water at different initial velocities, to accelerate or decelerate to their terminal velocity; 2) to assess whether different deployment heights may create a depth offset; and 3) to evaluate whether the currently used FRE coefficients also apply to the first 11 m of the descent.

This work represents the first attempt to experimentally verify the theoretically derived descent rate of XBT probes in the first meters in the water and to assess the physical mechanisms that create a depth offset in XBT profiles. This manuscript is organized as follows. The experimental setups and the methodology used to analyze the experimental data are described in section 2. Section 3 contains the results and the discussion, including the proposed correction of the FRE estimates for deployments made from different heights. The concluding remarks are presented in section 4.

2. Experimental setups

Two experiments were conducted to study the dynamics of the Sippican Deep Blue XBT probes during

the first 11 m of descent after the probes enter the water. The experiments were designed to assess the vertical displacements of the probes as a function of time, $z(t)$, for different deployment heights, and to determine the time that it takes the probes to reach their terminal vertical velocity in the water as a function of the deployment height.

The first experiment was carried out in a swimming pool 5 m deep at the University of Miami. A digital camera with a frame rate of 1/30s was installed at 1 m above the bottom of the pool and a rope with marks every 1 m was placed in the pool and used in the calibration of the recorded videos to determine the depth of the XBTs. During this experiment, XBTs were deployed with a straight orientation (vertically aligned facing down) from heights of 3 and 5 m above the surface of the water. These experimental vertical displacements were compared against those derived from the FRE estimates, using the coefficients proposed by H95 in (1) and (2), which provide the depth of the XBT in meters when the time is expressed in seconds.

The second experiment was conducted in a water tank 11.12 m tall at the NOAA National Data Buoy Center laboratory. To obtain a recording of the complete XBT trajectory, four digital cameras, each with a frame rate of 1/30s, were installed at 1.52-, 4.27-, 7.0-, and 9.75-m depth. These depths were selected because of the logistics to work inside the water tank and to ensure overlaps in the images between the videos produced by adjacent cameras. A vertical rope with markings every 1 m was placed in the water tank and used in the calibration of the recorded videos to determine the depth of the XBTs. During this experiment, XBTs were deployed in a straight orientation from heights of 0, 2, 4, 9, 14, 20, and 25 m.

In total, 135 deployments were carried out from nine different heights. The recordings obtained from both experiments were analyzed frame by frame using the software Tracker (Brown 2012) to obtain the values of the vertical position as a function of time. All deployments were repeated 15 times, and a third-degree polynomial was used to estimate the mean $z(t)$ for each deployment height. These fitted polynomials were then used to compute the vertical velocity in the water as a function of time for each deployment height.

The images analyzed in this study correspond to XBTs that fall in an orthogonal plane in front of the camera. In the analysis of the images, the first frame where the XBT was visible inside the water was used as the initial position ($t = 0$) of its vertical location. Thus, a linear interpolation of the data from different deployments was performed in order to obtain results that correspond to the same reference. In the second experiment, the videos had to be further calibrated to obtain a single

trajectory $z(t)$ from the recording of the four cameras used. The experimental values of the vertical trajectories were then compared to the H95 FRE and also used to validate the HT92 model.

3. Results

a. Deployment height and the first meters of descent

The experiments reported here were designed to investigate the effect of the deployment height on the fall rate during the first meters of the XBT descent in the water. During these experiments, XBT probes were deployed in a 5-m-deep pool and in an 11.12-m-deep water tank, as described in section 2. The XBTs were released from different heights and with a vertically straight orientation, with the objective of determining the deviation of the actual fall in the water from the H95 FRE estimates. In addition, these observations were used to assess the maximum depth at which these probes reach terminal velocity.

The difference between the actual fall and the H95 FRE estimates are shown in Fig. 1. Results indicate that XBTs deployed at the surface of the water ($h_0 = 0$), which also correspond to an initial velocity $w_0 = 0$, moved slower than the FRE estimates after entering the water. On the other hand, when the height of deployment was larger than $h_0 = 9$ m, the probes moved faster than the FRE estimates in the first upper meters. Small differences between the experimental results and the FRE estimates during the first 11 m were found for probes deployed from heights $2 \text{ m} \leq h_0 \leq 4 \text{ m}$. For deployments up to 20-m height, results show that the probes reach terminal velocity within the first 11 m. For deployment heights of 25 m, the probes did not reach terminal velocity in the first 11 m; however, their speed of descent indicated that they were approaching terminal velocity. Results show that while the vertical displacement of XBTs deployed from heights $2 \text{ m} \leq h_0 \leq 4 \text{ m}$ approximately coincides with the FRE estimates, displacement of probes deployed outside this range do not agree with those obtained from the H95 FRE. Therefore, this result indicates that the depth in profiles obtained from deployments made from heights $h_0 \leq 2 \text{ m}$ and $h_0 \geq 4 \text{ m}$ needs to be corrected during the first 2 s after the probe enters the water and until it reaches terminal velocity. If this depth error is not corrected, it will be carried over through the entire depth of the XBT temperature profile.

The H95 FRE implies an almost constant velocity of the probes during the entire fall in the water with only a very small deceleration as a result of the wire payout, which is given by the coefficient b in (1). Therefore, the

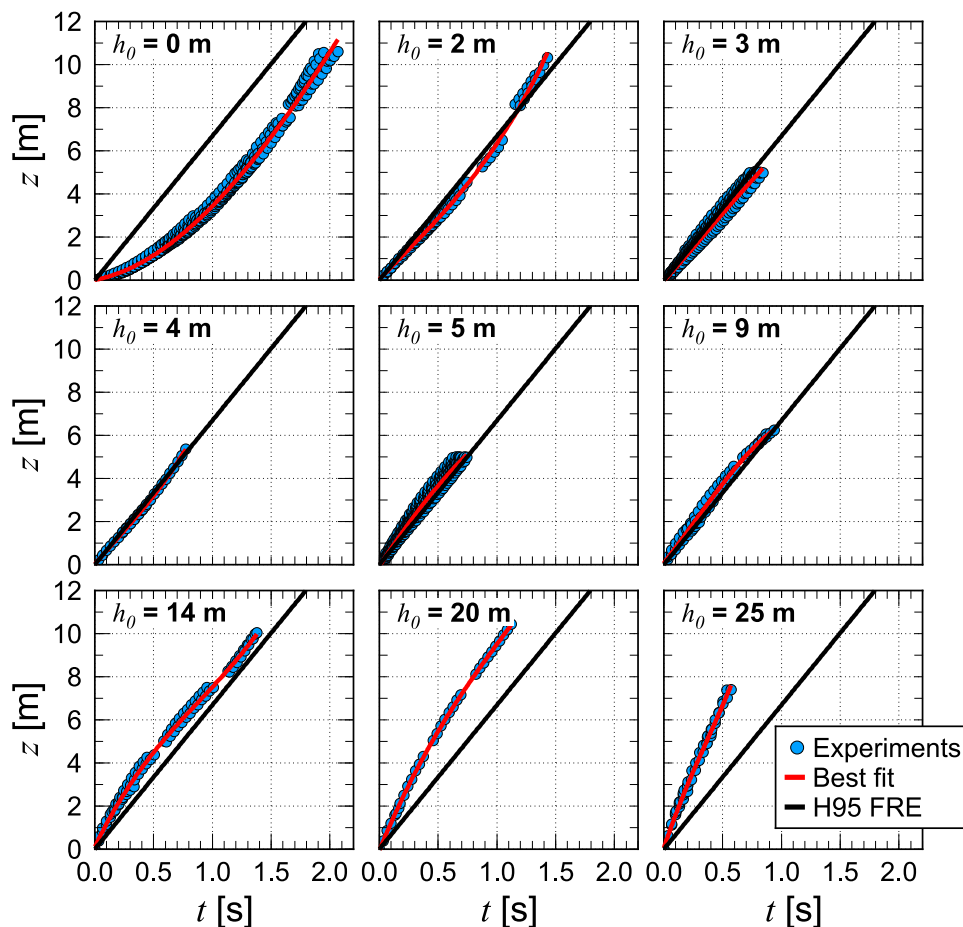


FIG. 1. Vertical position as a function of time for Deep Blue XBT probes deployed from different heights (blue circles), FRE estimates (black line), and third-order polynomial best fit of the experimental data (red line).

deployment of probes from different heights, which implies different initial velocities of the XBTs in the water, produced vertical displacements that were different from those estimated by the H95 FRE at the beginning of the fall. Results show that after entering the water, the XBTs accelerated (decelerated) from initial velocities, which were smaller (larger) than $a = 6.691 \text{ m s}^{-1}$, until their terminal velocity reached a value w_T that was equal or very close to a . From that instant, the probes continued to move at a rate close to the one described by (1) using the coefficients in (2). The results presented here (Fig. 1) show this behavior for all deployment heights under 25 m. For deployment heights of 25 m, the depth of the water tanks used in the experiment did not allow for the XBT probes to fully reach terminal velocities.

b. The initial velocity of descent

The initial velocity of descent of the XBT probes in the water depends on the velocity of impact of the

probes in the water, which is a function of the deployment height. We present here experimental results on the reduction of the velocity of the probes deployed 2 m and above the surface after they hit the water. The velocity of the probes at the instant of water impact, or velocity of free fall w_{ff} is

$$w_{\text{ff}} = \sqrt{2gh_0}, \quad (3)$$

where $g = 9.81 \text{ m s}^{-2}$ is the gravity acceleration and h_0 is the height of deployment. The velocity at the instant of water impact is compared here with the initial velocity of the probe in the water immediately after impact, which is estimated using the first two or three frames of the videos recorded during both experiments. Results are presented in Table 1 and in Fig. 2. Figure 2 shows that after the XBTs hit the water, their velocities quickly decrease as a result of the impact, unless they are deployed from $h_0 = 0$. This decrease in velocity

TABLE 1. Theoretical free fall velocity w_{ff} estimated as a function of the deployment height h_0 and observed initial velocity w_0 of the XBTs in the water. The difference $\Delta w = w_{ff} - w_0$ indicates the loss of momentum of the probes upon impact in the water.

h_0 (m)	w_{ff} (m s^{-1})	w_0 (m s^{-1})	Δw (m s^{-1})
2	6.26	5.73 ± 0.42	0.53 ± 0.42
3	7.67	6.40 ± 0.55	1.27 ± 0.55
4	8.86	6.86 ± 0.18	2.00 ± 0.18
5	9.90	8.23 ± 0.72	1.67 ± 0.72
9	13.29	9.78 ± 1.40	3.51 ± 1.40
14	16.57	12.47 ± 1.25	4.10 ± 1.25
20	19.81	16.04 ± 1.83	3.77 ± 1.83
25	22.14	17.05 ± 0.54	5.09 ± 0.54

(Δw) is proportional to the deployment height h_0 . Although the results shown in Fig. 2 do not suggest a linear relationship between Δw and h_0 , we expect a continuous increase of Δw with the height of deployment in most applications, where XBTs are deployed from $h_0 < 35$ m. The observed initial velocities of the XBTs in the water (Fig. 3) were determined for deployment heights between 0 and 25 m (an initial velocity $w_0 = 0$ is assumed for $h_0 = 0$) (Table 1). Currently, the most commonly used XBT probes, the Deep Blues, are manufactured to be deployed from heights of 3–4 m above the sea surface and have been reported to produce initial velocities in the water of 6–7 m s^{-1} (NOAA 2014, codes 51 and 52), which is confirmed by our experiments. Therefore, probes deployed from the height interval of 3–4 m (gray area in Fig. 3) will not introduce a depth bias in the FRE of the form (1) and will not require an offset correction because of deployment height.

To obtain the initial velocity of the XBTs as a function of the height of deployment, an exponential function of the form

$$w_0(h_0) = ph_0^q \quad (4)$$

was fitted to the experimental data (Fig. 3), obtaining the following values for the parameters: $p = 3.7066$ and $q = 0.4745$.

Results obtained here indicate that for a deployment height of 1 m, XBTs will start their descent in the water at 3.7 m s^{-1} , which is lower than the XBT terminal velocity of 6.691 m s^{-1} . These probes will accelerate for several meters until they reach their terminal velocity. The consequence of not considering this effect is that the XBT depth estimates are deeper than the actual depths of the XBTs. On the other hand, for a deployment height of 15 m, XBTs will start their descent at 13.4 m s^{-1} , which is larger than the terminal velocity, and will decelerate for several meters until they reach their terminal velocity. The consequence of not considering

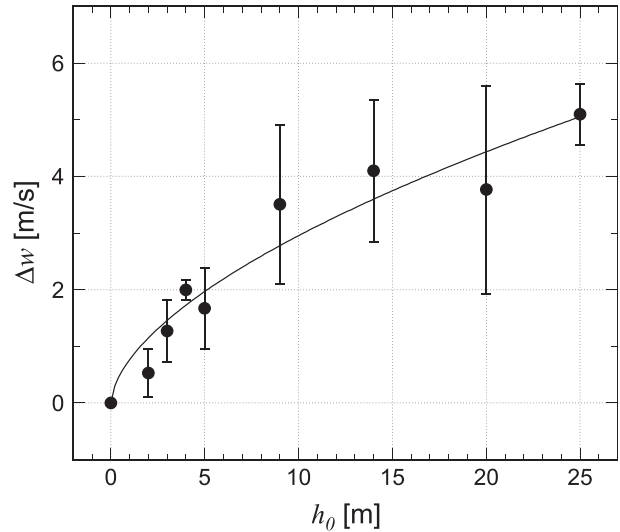


FIG. 2. Difference between the velocity of the probes before and after impact in the water as a function of the deployment height.

this effect is that the XBT depth estimates are shallower than the actual depth of the XBTs.

A correction to the FRE that can account for the deviations from a constant velocity of descent (Fig. 1) should therefore include the initial velocity in the water. Since this value cannot be obtained during normal XBT deployments, Fig. 3 and (4) provide a method to estimate this initial velocity as a function of the deployment height, a parameter that is measurable.

c. FRE correction as a function of deployment height

The fall-rate equation of an XBT can be obtained theoretically assuming a balance between the vertical acceleration, the total buoyancy force, and the hydrodynamic drag, which is considered proportional to the square of the velocity of descent in the water (Green 1984):

$$\frac{d^2z}{dt^2} = \frac{g(m - m_w)}{m} - \frac{\rho_w C_D A w^2}{2m}, \quad (5)$$

where z is the vertical position (positive downward), t is time, g is the acceleration of gravity, m is the mass of the XBT probe, m_w is the mass of displaced water, ρ_w is the water density, C_D is the drag coefficient, A is the effective cross section (area) of the probe, and w is the vertical velocity (positive downward). Equation (5) can be integrated by a parameterization of varying magnitudes, $m - m_w$ and C_D , and by considering a negligible acceleration, $d^2z/dt^2 \simeq 0$, to obtain (Green 1984)

$$z(t) = w_T t - \frac{\eta w_T^2 t^2}{4}, \quad (6)$$

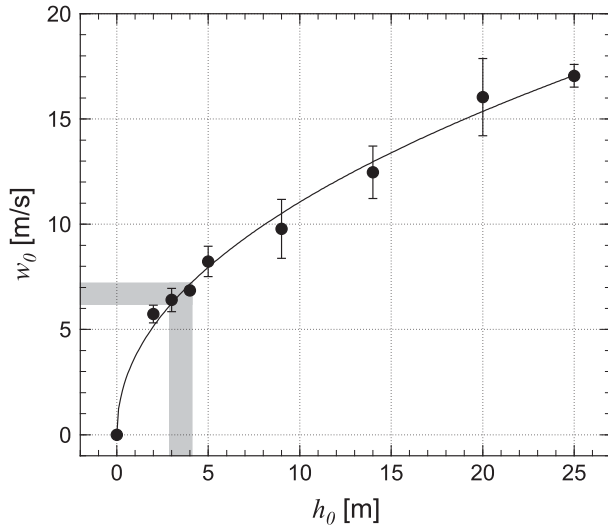


FIG. 3. Experimental values of the initial velocity of the XBT in the water (w_0) as a function of the deployment height h_0 . The black curve is a nonlinear fit of the function $w_0(h_0) = ph_0^q$, with $p = 3.7066$ and $q = 0.4745$. XBTs deployed from a height within the gray area will have initial velocity in the water close to the terminal velocity.

which is the fall-rate equation in the form of (1), with

$$\begin{aligned} w_T &= a, \\ \frac{\eta w_T^2}{4} &= b, \end{aligned} \quad (7)$$

and η is a parameter used to account for the linear variations assumed for C_D and the mass decrease as a result of the wire payout as a function of depth. The nature of the parameters m_w , C_D , and ρ_w in (5) may vary for different geographical regions but are assumed to be constant in this work. Additionally, m , C_D , m_w , and ρ_w vary with depth. The physical meaning of the solution (6) obtained for (5) indicates that the probe is expected to have a motion in which the acceleration, the left-hand side of (5), is very small and that the probe falls at an almost constant w_T throughout the entire water column, including at the beginning of the descent. However, the results presented in the previous section show that the descent of an XBT exhibits different initial velocities after entering the water, which depend on the deployment height, until it reaches w_T .

A model proposed by HT92 for the fall of the XBT in the first 10 m in the water is intended to account for the difference between the actual velocity of the XBT at the beginning of its descent and w_T . For $z \leq 10$ m ($t \leq 1.5$ s), the contribution of the quadratic term in (5) is very small, approximately 0.5 cm, and therefore (5) can be simplified by considering that the parameters in this equation are constant while including the vertical acceleration, to obtain

$$\frac{d^2z}{dt^2} = \frac{dw}{dt} = \beta - \alpha w^2, \quad (8)$$

where

$$\alpha = \frac{\rho_w C_D A}{2m}, \quad (9)$$

$$\beta = \frac{gm'}{m}, \quad (10)$$

and m' is the weight of the XBT in the water. Since $d^2z/dt^2 = 0$ when the XBT velocity of descent (w) reaches its terminal velocity (w_T), from (8) it is obtained,

$$w_T = \sqrt{\frac{\beta}{\alpha}} = \sqrt{\frac{2gm'}{\rho_w C_D A}}. \quad (11)$$

Equation (8) can be written in terms of the vertical velocity and integrated twice to obtain $w = w(t)$ and $z = z(t)$, using the initial conditions $w(0) = w_0$ and $z(0) = 0$. The result for $z(t)$ is obtained as

$$z_1(t, w_0) = \frac{1}{\alpha} \left\{ \begin{array}{l} \ln \left[\frac{\sinh(\alpha w_T t + C_1)}{\sinh C_1} \right]; \frac{w_0}{w_T} > 1 \\ \ln \left[\frac{\cosh(\alpha w_T t + C_2)}{\cosh C_2} \right]; \frac{w_0}{w_T} < 1 \end{array} \right\}, \quad (12)$$

where $C_1 = \coth^{-1}(w_0/w_T)$ and $C_2 = \tanh^{-1}(w_0/w_T)$.

Using the experimental results obtained in this work, we can validate the theoretical model above for the vertical position of the XBT during the first 11 m of descent as given by (12). The differences between the FRE using the coefficients of H95 and the observed vertical displacements for different deployment heights are presented in Fig. 4, together with the difference between the fall-rate equation of H95 and the solution obtained using HT92 [(12)], with $w_T = 6.691 \text{ m s}^{-1}$; $g = 9.80665 \text{ m s}^{-2}$; $\alpha = 0.16623 \text{ m}^{-1}$, determined from

$$\alpha = \frac{gm'}{mw_T^2}, \quad (13)$$

where $m'/m = 0.75888$; and the initial velocity of descent w_0 from Table 1.

The differences between the H95 FRE and the observed vertical positions, and the H95 FRE and the HT92 model, are shown in Fig. 4, using the experimental values of w_0 from Table 1. Results show that for $h_0 = 4$ m, these differences are very small (on average $0.04 \text{ m} \pm 0.02 \text{ m}$). These differences are larger for deployment heights below and above 4 m, consistent with the results already presented in Fig. 1. An important result obtained here is that since the differences between

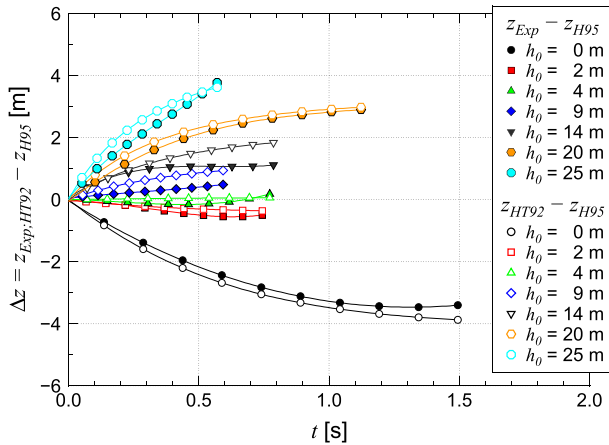


FIG. 4. Difference between the observed depth z_{Exp} and the H95 FRE z_{H95} (solid symbols) and the depth from the HT92 model z_{HT92} and z_{H95} (open symbols) for different heights of deployment h_0 .

the observed positions and H95 are very similar to those between HT92 and H95, then HT92 provides a very good description of the observed descent of the probes during the first meters. In particular, while differences of as much as 15% can be observed between the experimental observations and HT92, both compare very well for the extreme deployment heights of 0 and 20–25 m.

The model in HT92 provides a solution [(12)] for the depth of the XBT during the first 10–15 m ($t \leq 1.5$ s) of descent as a function of the initial velocity of the probe in the water.

Since (12) was obtained by disregarding the contribution of the quadratic term at the beginning of the descent, a general FRE can be proposed by adding the quadratic term in (6) to the solution [(12)] to obtain (HT92)

$$z(t) = z_1(t, w_0) - \underbrace{\frac{\eta w_T^2 t^2}{4}}_{\substack{\cong 0 \text{ for } t \leq 1.5 \text{ s} \\ t > 0}}, \quad (14)$$

where $z_1(t, w_0)$ is given by (12). Equation (14) is the general FRE that should be used to eliminate the depth offset resulting from varying deployment heights.

It can be shown that for sufficiently large times ($t > 1.5$ s),

$$z_1(t) = w_T t + D, \quad (15)$$

where D is the maximum offset in the temperature profile resulting from the deployment height. Therefore, for sufficiently large times ($t > 1.5$ s) (14) approaches the form

$$z(t) = at - bt^2 + D, \quad (16)$$

where a, b are defined in (1). Given a FRE in the form of (1), the new depth can be estimated from (14) provided that the initial velocity of the probe in the water is known. In most practical situations and for Deep Blue XBTs, the initial velocity can be obtained from (4) if the height of deployment is known. This is a parameter that can be estimated during an XBT deployment. This result indicates that by using H95 [(1), (2)], the depth offset will always exist unless the XBT is deployed from heights between 3 and 4 m (gray area in Fig. 3).

The methodology proposed in this work to correct the depth offset caused by different deployment heights in temperature profiles obtained from Deep Blue XBT probes with an FRE of the type (1) is as follows:

- 1) The initial velocity of the XBTs in the water (w_0) is estimated using (4).
- 2) The initial (w_0) and terminal [w_T ; i.e., coefficient a in the FRE of the type (1)] velocities of the XBTs in the water are used to compute $z_1(t, w_0)$ using (12).
- 3) Here $z_1(t, w_0)$ and the coefficient b of the FRE of the type (1) are used to compute the new depth as a function of time using

$$z(t) = z_1(t, w_0) - bt^2. \quad (17)$$

As an example, Fig. 5 shows how the proposed methodology estimates the depth of an XBT when different heights of deployments are considered. The temperature profile in this example (Fig. 5a) was obtained at location 32.71°N, 46.03°W on 19 March 2014 from an XBT deployed from a height of approximately 10 m. This profile is characterized by a mixed layer depth of approximately 21°C to 150 m, a pronounced thermocline between 150 and 200 m, and a smaller monotonic negative temperature gradient between 200 and 800 m. After the methodology proposed here is applied, a depth offset is removed from the original profile. Depending on the deployment height, different probe depths are estimated for one given time. Differences between H95 and the observed depths are closer to zero for $h_0 = 3$ m (Fig. 5b). These differences are negative (positive) for deployment heights below (above) 3 m (Fig. 5b). In this example, the depth offset for a deployment height of 10 is 2 m. Also, differences between the profiles before and after the offset correction (Fig. 5c) for this specific deployment made from a deployment height of 10 m show that the temperature differences are 1) between 0° and -0.1°C within the mixed layer; 2) up to -0.6°C in the thermocline, at

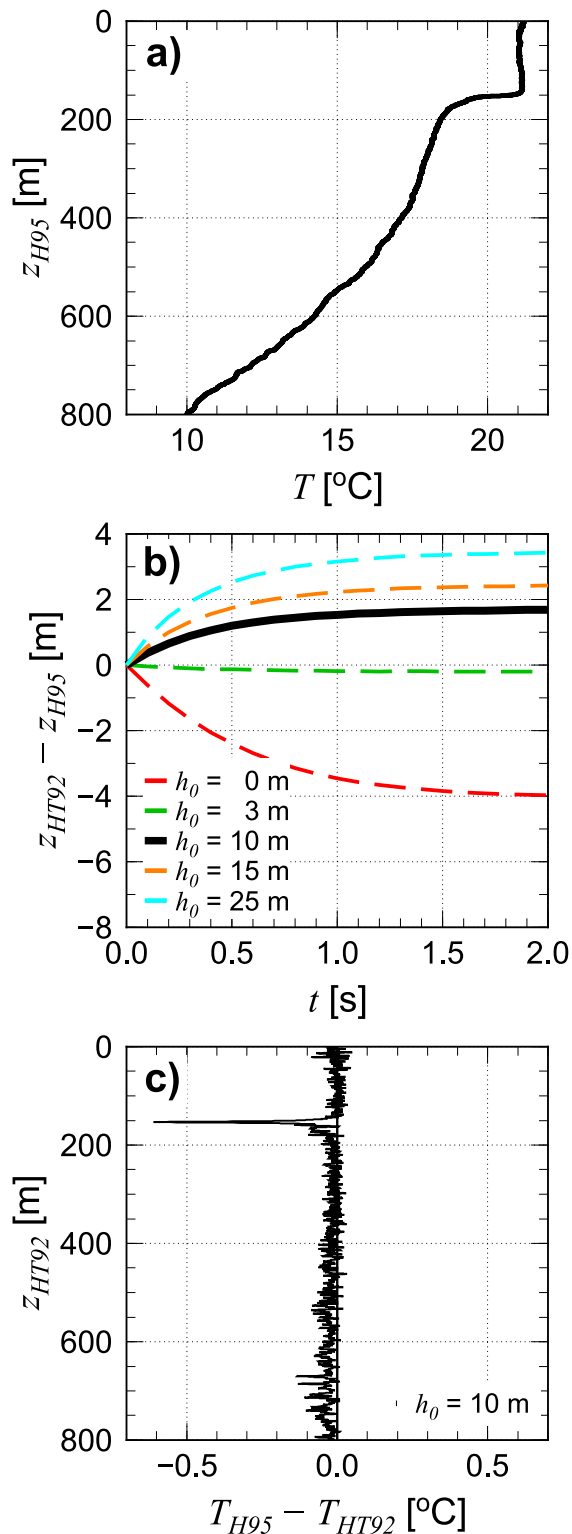


FIG. 5. Example of depth offset correction of an XBT profile. (a) Original XBT profile. (b) Depth difference as a function of time between the original (H95) and the corrected (using HT92) profiles during the first 1.5 s for several deployment heights. (c) Temperature difference as a function of depth between the original (H95) and the corrected (using HT92) profile for a deployment height of 10 m.

approximately 150 m deep; and 3) between 0° and 0.15°C below the thermocline. Depth offsets produced in profile data, such as the one described above, have large errors in depth estimates at the depth of large temperature gradients. For the case above, the offset produces an excess of heat above the 18°C isotherm of 2.5 kJ cm^{-2} . This indicates that the depth offset may have a noticeable impact on upper-ocean heat content computations.

Following the results presented above, temperature profiles obtained using H95 need to be adjusted by converting time into depth, where the depth is determined using (17), which is a function of w_0 , w_T , and time; w_0 is determined by (4), which is a function of the deployment height; and w_T is given by the coefficient a in (2).

d. Maximum offset in the FRE estimates

The methodology described in this work estimates the offset to be removed from the profile computed using any FRE of the form (1). For times $t < 1.5$ s, the depth offset is a function of time and is given by the difference between the FRE used and (12). For $t > 1.5$ s the XBT is already moving at terminal velocity and the offset is constant. During the transition period until the XBT reaches w_T , this offset is introduced as the FRE (1) considers that the XBT is moving at terminal velocity since the beginning of the descent. The results in Fig. 4 can be used to estimate the time at which w_T is reached. This time is when the maximum value of Δz is reached between the experimental $z(t)$ and the estimates of the H95 FRE. At this moment, D has been reached and the XBT is moving with terminal velocity.

The values of D introduced in the FRE as observed in our experiments are presented in Fig. 6 and Table 2. This offset depends on the deployment height, being approximately equal to zero for deployments done from heights between 3 and 4 m and negative (positive) for deployments from heights below (above) these values. Figure 6 shows that during common XBT deployments from cargo ships, where the height of deployment can be between 10 and 35 m, a depth offset of more than 3.7 m may be introduced in the profiles computed using H95 FRE. Table 2 and Fig. 6 are only provided here in order to illustrate the maximum magnitude of D resulting from different deployment heights. Since this depth offset is a function of time, the actual profile depth with the offset removed should be computed using the methodology described above [based on Eq. (17)].

4. Summary and conclusions

Two experiments were conducted in order to assess the effect of the deployment height in the fall rate of Deep Blue XBT probes in the water. Experimental

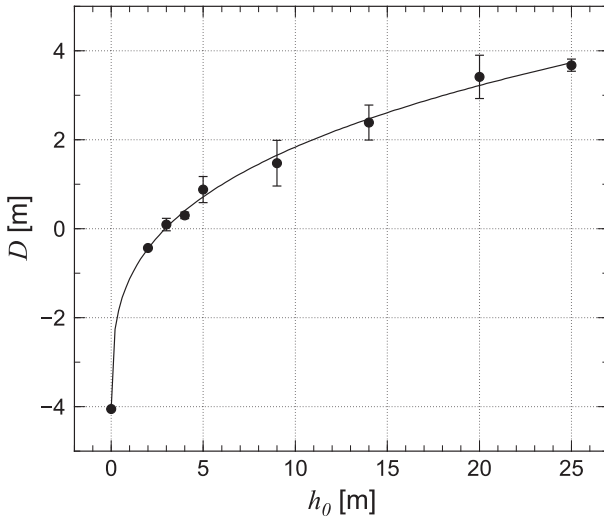


FIG. 6. Maximum offset D observed in the depth of XBT probes when using the H95 FRE without considering a correction for the deployment height.

results confirmed theoretical studies in which there is a depth offset in the XBT FRE that depends on the height of deployment. This offset ranges from approximately -4 to 4 m depending on the deployment height. This offset is time dependent during the first 1.5 s of descent in the water and constant after that. To eliminate the offset during the first 1.5 s of descent, a theoretical model (HT92) was shown to provide an adequate estimate of the actual depth of the XBT.

To correct the depth of a Deep Blue XBT profile obtained using a FRE of the type $z(t) = at - bt^2$ —for example, the H95 equation, (17), can be used with $z_1(t, w_0)$ given by (12)— $\alpha = 0.16623 \text{ m}^{-1}$, $w_T = a$, and $w_0(h_0) = ph_0^q$, with parameters $p = 3.7066$ and $q = 0.4745$ that were obtained empirically on this work (sections 3b and 3c). This correction applies to any FRE of the type (1) and assumes that the coefficients a and b are representative of the correct form of the XBT FRE after the probe has reached its terminal velocity.

We recommend that the correction proposed here be used to improve the historical XBT database and be applied to current observations, provided that the deployment height is known. Although the deployment height is not always known, it could be inferred from the metadata containing information on the ships from which the deployments were performed. For research ships the typical deployment height ranges from 2 to 5 m, while for cargo ships it ranges from 10 to 35 m. In addition, for XBTs deployed using automatic launchers, which include most XBT deployments in high-density mode since 1997, typical deployment heights are between 10 and 15 m. For deployments carried out from

TABLE 2. Maximum offset D in the H95 FRE observed during this work for different deployment heights h_0 .

h_0 (m)	D (m)
0	-4.05
2	-0.44
3	0.03
4	0.40
5	0.72
9	1.65
14	2.47
20	3.22
25	3.73

cargo ships in low-density mode or frequently repeated mode, deployments are mostly made from typical heights between 15 and 35 m.

Results presented here are independent of the FRE, XBT recording system, and sea state, among other parameters, because they are based on direct observations of XBT positions as a function of time. Therefore, the depth offset described and assessed here is purely due to the effect of initial velocities on XBT depth estimates caused by different launch heights. However, other factors, including the potential effect of varying ship speeds, water entry conditions, ocean conditions, acquisition and recording system, water density, temperature, etc., may also contribute to the depth offset and will need to be assessed. Our results highlight the need of continuous improvements in observational datasets. This work was specifically carried out for Sippican Deep Blue XBT probes, and similar experiments, studies, and analysis should be performed for other types of probes. Studies such as this one contribute to reducing the error in global ocean heat content estimates by improving the quality of historical datasets, especially during the period 1969–2001, when XBTs accounted for most of the temperature profile data.

Acknowledgments. The authors would like to acknowledge Grant Rawson, Pedro Pena, and Kyle Seaton for their work during the execution of the experiments presented here, as well as Zach Barton for the help provided tracking the movement of the XBTs in the videos. We would also like to acknowledge the support of NOAA’s National Marine Fisheries Service and Southeast Fisheries Science Center during these experiments. This work was supported by NOAA’s Climate Program Office and NOAA AOML.

REFERENCES

Abraham, J. P., J. M. Gorman, F. Reseghetti, E. M. Sparrow, and W. J. Minkowycz, 2012a: Drag coefficients for rotating expendable bathythermographs and the impact of launch

- parameters on depth predictions. *Numer. Heat Transfer*, **62A**, 25–43, doi:10.1080/10407782.2012.672898.
- , —, —, —, and —, 2012b: Turbulent and transitional modeling of drag on oceanographic measurement devices. *Modell. Simul. Eng.*, **2012**, 567864, doi:10.1155/2012/567864.
- , and Coauthors, 2013: A review of global ocean temperature observations: Implications for ocean heat content estimates and climate change. *Rev. Geophys.*, **51**, 450–483, doi:10.1002/rog.20022.
- Arnault, S., B. Boulès, Y. Gouriou, and R. Chuchla, 1999: Intercomparison of the upper layer circulation of the western equatorial Atlantic Ocean: In situ and satellite data. *J. Geophys. Res.*, **104**, 21 171–21 194, doi:10.1029/1999JC900124.
- , I. Pujol, and J. L. Melice, 2011: In situ validation of Jason-1 and Jason-2 altimetry missions in the tropical Atlantic Ocean. *Mar. Geod.*, **34**, 319–339, doi:10.1080/01490419.2011.584833.
- Baringer, M. O., and S. L. Garzoli, 2007: Meridional heat transport determined with expendable bathythermographs—Part I: Error estimates from model and hydrographic data. *Deep-Sea Res. I*, **54**, 1390–1401, doi:10.1016/j.dsr.2007.03.011.
- Brown, D., 2012: Tracker: Video analysis and modeling tool for physics education. [Available online at <http://www.cabrillo.edu/~dbrown/tracker/>]
- Carton, J. A., and E. J. Katz, 1990: Estimates of the zonal slope and seasonal transport of the Atlantic North Equatorial Counter-current. *J. Geophys. Res.*, **95**, 3091–3100, doi:10.1029/JC095iC03p03091.
- Cheng, L., and Coauthors, 2015: XBT science: Assessment of instrumental biases and errors. *Bull. Amer. Meteor. Soc.*, doi:10.1175/BAMS-D-15-00031.1, in press.
- Cowley, R., S. Wijffels, L. Cheng, T. Boyer, and S. Kizu, 2013: Biases in expendable bathythermograph data: A new view based on historical side-by-side comparisons. *J. Atmos. Oceanic Technol.*, **30**, 1195–1225, doi:10.1175/JTECH-D-12-00127.1.
- DiNezio, P. N., and G. G. Goni, 2010: Identifying and estimating biases between XBT and Argo observations using satellite altimetry. *J. Atmos. Oceanic Technol.*, **27**, 226–240, doi:10.1175/2009JTECH0711.1.
- , and G. J. Goni, 2011: Direct evidence of a changing fall-rate bias in XBTs manufactured during 1986–2008. *J. Atmos. Oceanic Technol.*, **28**, 1569–1578, doi:10.1175/JTECH-D-11-00017.1.
- Domingues, R., G. J. Goni, S. Swart, and S. Dong, 2014: Wind forced variability of the Antarctic Circumpolar Current south of Africa between 1993 and 2010. *J. Geophys. Res. Oceans*, **119**, 1123–1145, doi:10.1002/2013JC008908.
- Dong, S., S. Garzoli, M. Baringer, C. Meinen, and G. Goni, 2009: Interannual variations in the Atlantic meridional overturning circulation and its relationship with the net northward heat transport in the South Atlantic. *Geophys. Res. Lett.*, **36**, L20606, doi:10.1029/2009GL039356.
- , M. O. Baringer, G. J. Goni, C. S. Meinen, and S. L. Garzoli, 2014: Seasonal variations in the South Atlantic Meridional Overturning Circulation from observations and numerical models. *Geophys. Res. Lett.*, **41**, 4611–4618, doi:10.1002/2014GL060428.
- Gilson, J., D. Roemmich, B. Cornuelle, and L.-L. Fu, 1998: Relationship of TOPEX/Poseidon altimetric height to steric height and circulation in the North Pacific. *J. Geophys. Res.*, **103**, 27 947–27 965, doi:10.1029/98JC01680.
- Goes, M., G. Goni, V. Hormann, and R. C. Perez, 2013: Variability of the Atlantic off-equatorial eastward currents during 1993–2010 using a synthetic method. *J. Geophys. Res. Oceans*, **118**, 3026–3045, doi:10.1002/jgrc.20186.
- , M. Baringer, and G. Goni, 2015: The impact of historical biases on the XBT-derived meridional overturning circulation estimates at 34°S. *Geophys. Res. Lett.*, **42**, 1848–1855, doi:10.1002/2014GL061802.
- Goni, G., S. Kamholtz, S. Garzoli, and D. Olson, 1996: Dynamics of the Brazil-Malvinas Confluence based on inverted echo sounders and altimetry. *J. Geophys. Res.*, **101**, 16 273–16 289, doi:10.1029/96JC01146.
- Gourcuff, C., P. Lherminier, H. Mercier, and P.-Y. LeTraon, 2011: Altimetry combined with hydrography for ocean transport estimation. *J. Atmos. Oceanic Technol.*, **28**, 1324–1337, doi:10.1175/2011JTECH0818.1.
- Gouretski, V., and K. P. Koltermann, 2007: How much is the ocean really warming? *Geophys. Res. Lett.*, **34**, L01610, doi:10.1029/2006GL027834.
- , and F. Reseghetti, 2010: On depth and temperature biases in bathythermograph data: Development of a new correction scheme based on analysis of a global ocean database. *Deep-Sea Res. I*, **57**, 812–833, doi:10.1016/j.dsr.2010.03.011.
- Green, A. W., 1984: Bulk dynamics of the expendable bathythermograph (XBT). *Deep-Sea Res.*, **31**, 415–426, doi:10.1016/0198-0149(84)90093-1.
- Hallock, Z. R., and W. J. Teague, 1992: The fall rate of the T-7 XBT. *J. Atmos. Oceanic Technol.*, **9**, 470–483, doi:10.1175/1520-0426(1992)009<0470:TFROTT>2.0.CO;2.
- Hamon, M., G. Reverdin, and P.-Y. Le Traon, 2012: Empirical correction of XBT data. *J. Atmos. Oceanic Technol.*, **29**, 960–973, doi:10.1175/JTECH-D-11-00129.1.
- Hanawa, K., and H. Yoritaka, 1987: Detection of systematic errors in XBT data and their correction. *J. Oceanogr. Soc. Japan*, **43**, 68–76, doi:10.1007/BF02110635.
- , P. Rual, R. Bailey, A. Sy, and M. Szabados, 1995: A new depth time equation for Sippican or TSK T-7, T-6 and T-4 expendable bathythermographs (XBT). *Deep-Sea Res. I*, **42**, 1423–1451, doi:10.1016/0967-0637(95)97154-Z.
- Heinmiller, R. H., C. C. Ebbesmeyer, B. A. Taft, D. B. Olson, and O. P. Nikitin, 1983: Systematic errors in expendable bathythermograph (XBT) profiles. *Deep-Sea Res.*, **30A**, 1185–1197, doi:10.1016/0198-0149(83)90096-1.
- Ishii, M., and M. Kimoto, 2009: Reevaluation of historical ocean heat content variations with time-varying XBT and MBT depth bias corrections. *J. Oceanogr.*, **65**, 287–299, doi:10.1007/s10872-009-0027-7.
- Kizu, S., C. Sukigara, and K. Hanawa, 2011: Comparison of the fall rate and structure of recent T-7 XBT manufactured by Sippican and TSK. *Ocean Sci.*, **7**, 231–244, doi:10.5194/os-7-231-2011.
- Levitus, S., J. I. Antonov, T. P. Boyer, R. A. Locarnini, H. E. Garcia, and A. V. Mishonov, 2009: Global ocean heat content 1955–2008 in light of recently revealed instrumentation problems. *Geophys. Res. Lett.*, **36**, L07608, doi:10.1029/2008GL037155.
- NOAA, 2014: WMO code table 1770. [Available online at <https://www.nodc.noaa.gov/GTSP/Document/codetbls/wmocodes/table1770.html>.]
- Phillips, H. E., and S. R. Rintoul, 2002: A mean synoptic view of the sub-Antarctic front south of Australia. *J. Phys. Oceanogr.*, **32**, 1536–1553, doi:10.1175/1520-0485(2002)032<1536:AMSVOT>2.0.CO;2.
- Reseghetti, F., M. Borghini, and G. M. R. Manzella, 2007: Factors affecting the quality of XBT data—Results of analysis on profiles from the western Mediterranean Sea. *Ocean Sci.*, **3**, 59–75, doi:10.5194/os-3-59-2007.

- Ridgway, K. R., R. C. Coleman, R. J. Bailey, and P. Sutton, 2008: Decadal variability of East Australian Current transport inferred from repeated high-density XBT transects, a CTD survey and satellite altimetry. *J. Geophys. Res.*, **113**, C08039, doi:10.1029/2007JC004664.
- Rintoul, S. R., S. Sokolov, and J. Church, 2002: A 6 year record of baroclinic transport variability of the Antarctic Circumpolar Current at 140°E derived from expendable bathythermograph and altimeter measurements. *J. Geophys. Res.*, **107**, 3155, doi:10.1029/2001JC000787.
- Roemmich, D., and B. Cornuelle, 1987: Digitization and calibration of the expendable bathythermograph. *Deep-Sea Res.*, **34A**, 299–307, doi:10.1016/0198-0149(87)90088-4.
- , J. Gilson, B. Cornuelle, and R. Weller, 2001: Mean and time-varying meridional transport of heat at the tropical/subtropical boundary in the North Pacific Ocean. *J. Geophys. Res.*, **106**, 8957–8970, doi:10.1029/1999JC000150.
- Seaver, G. A., and S. Kuleshov, 1982: Experimental and analytical error of expendable bathythermograph. *J. Phys. Oceanogr.*, **12**, 592–600, doi:10.1175/1520-0485(1982)012<0592:EAAEOT>2.0.CO;2.
- Singer, J. J., 1990: On the error observed in electronically digitized T-7 XBT data. *J. Atmos. Oceanic Technol.*, **7**, 603–611, doi:10.1175/1520-0426(1990)007<0603:OTEIOE>2.0.CO;2.
- Smith, N. R., and Coauthors, 1999: The role of XBT sampling in the ocean thermal network. *Proc. OceanObs'99*, Saint Raphaël, France, Centre National d'Études Spatiales, 1–26.
- Thadathil, P., A. K. Saran, V. V. Gopalakrishna, P. Vethamony, N. Araligidad, and R. Bailey, 2002: XBT fall rate in waters of extreme temperature: A case study in the Antarctic Ocean. *J. Atmos. Oceanic Technol.*, **19**, 391–396, doi:10.1175/1520-0426-19.3.391.
- Wijffels, S. E., J. Willis, C. M. Domingues, P. Barker, N. J. White, A. Gronell, K. Ridgway, and J. A. Church, 2008: Changing expendable bathythermograph fall rates and their impact on estimates of thermohaline sea level rise. *J. Climate*, **21**, 5657–5672, doi:10.1175/2008JCLI2290.1.
- Xiao, H., and X. Zhang, 2012: Numerical investigations of the fall rate of a sea-monitoring probe. *Ocean Eng.*, **56**, 20–27, doi:10.1016/j.oceaneng.2012.08.002.
- , C. Liu, and J. Tao, 2006: Numerical simulation and experiments of a probe descending in the sea. *Ocean Eng.*, **33**, 1343–1353, doi:10.1016/j.oceaneng.2005.10.001.